Applied Physics Letters ARTICLE pubs.aip.org/aip/apl

Field-sensitivity and reversibility of the inverse magnetocaloric effect at martensitic transformations

Cite as: Appl. Phys. Lett. **124**, 052403 (2024); doi: 10.1063/5.0185552
Submitted: 31 October 2023 · Accepted: 12 January 2024 ·
Published Online: 31 January 2024

View Online Export Citation CrossMark

Chris Taake,[1] Tapas Samanta,[1,a)] and Luana Caron[1,2]

AFFILIATIONS

[1]Faculty of Physics, Bielefeld University, P.O. Box 100131, D-33501 Bielefeld, Germany
[2]Helmholtz-Zentrum Berlin für Materialien und Energie, Berlin 12489, Germany

[a)]Author to whom correspondence should be addressed: tapas.sinp@gmail.com and tsamanta@physik.uni-bielefeld.de

ABSTRACT

The magnetic field-sensitivity of martensitic phase transitions (MPTs) responsible for magnetocaloric effects has been examined in B-substituted $Ni_{50}Mn_{34.8}In_{15.2-x}B_x$ Heusler alloys ($x = 1$, 2, 3, and 4). Increasing boron substitution acts as a positive chemical pressure similar to the effect of hydrostatic pressure (p) and shifts the martensitic phase transition temperature (T_M) toward higher temperature. The observed structural compatibility of the MPT results in a lower thermal hysteresis ($\Delta T_{hyst} < 5$ K at low field). ΔT_{hyst} remains almost unchanged; however, the field sensitivity of T_M decreases significantly with increasing B content or application of p. As a result, the reversibility of the isothermal entropy change ($|\Delta S_{rev}|$) reduces for higher B concentration or under hydrostatic pressure p. The experimental observation reveals that the lower field-sensitivity of the MPT with increasing B or p is associated with the simultaneous increase in the magnetocrystalline anisotropy energy (MAE) and decrease in the Zeeman energy (ZE). The relatively larger ZE and smaller MAE for $x = 1$ result in the improved reversibility of the entropy change ($|\Delta S_{rev}| = 21.48$ J/kg K for $\Delta\mu_0 H = 5$ T), which is comparable to or even larger than the values reported for similar Heusler alloys.

It is a well-established fact that a large change in magnetization resulting from the field-induced martensitic phase transition (MPT) in Ni–Mn–X (X = In and Sn) full Heusler alloys gives rise to giant magnetocaloric effects (MCE),[1] magnetoresistance properties,[2] magnetic shape memory effects,[3] and so on. In particular, the research on MCE is progressively increasing due to its possible application in greener magnetic refrigeration. In addition to Heusler alloys, some recently reported magnetocaloric materials fabricated from nontoxic cheaper elements, such as $Mn_{30}Fe_{20-x}Cu_xAl_{50}$ alloys[4] and transition metal-based high-entropy alloys,[5–7] have the potential to exhibit good MCE properties near room temperature. Moreover, newly developed rare-earth-based magnetocaloric materials are also proposed as promising candidates for cryogenic[8,9] as well as room-temperature[10] magnetic refrigeration. Chemical alloying,[11,12] stoichiometry changes,[13,14] and application of hydrostatic pressure[15,16] are the most common techniques adopted to optimize the above-mentioned functional properties. This type of optimization scheme can modify the nature of the field-induced MPT drastically. It is not even surprising to observe extreme kinds of phase transitions as described by Anzai and Ozawa,[17] where a first-order martensitic phase transition occurs for both order parameters (magnetization and crystal symmetry) simultaneously, but it is sensitive to one order parameter, while the other changes cooperatively. Therefore, this type of phase transition can be triggered more easily by one external parameter, i.e., field (can drive the magnetic transition) or pressure/temperature (can drive the structural transition). The temperature-induced MPT (where the temperature-induced structural transition drives the first-order phase transition, and the magnetic transition occurs cooperatively) is obviously not interesting for field-induced functional applications due to the low field-sensitivity of the phase transition. However, it is not clear how the nature of the field-induced MPT can be controlled in practice. Therefore, gaining a better understanding about the nature of the field-induced MPT is essential for applications.

In-based off-stoichiometric Heusler alloys undergo a MPT from a low-temperature low-moment martensitic phase (lower symmetry crystal structure than the austenitic phase, such as body-centered tetragonal, modulated monoclinic structure) to a high-temperature ferromagnetic (FM) austenitic phase (face-centered cubic structure).[18–20]

The field-sensitivity of the MPT mainly depends on the competition between the Zeeman energy (ZE) and the magnetocrystalline anisotropy energy (MAE) in the martensitic phase.[21] For a field-induced MPT to occur, the available ZE must be large enough to overcome the MAE. The Clausius Clapeyron equation $\Delta S = -\Delta M\left(\frac{\Delta T}{\Delta \mu_0 H}\right)^{-1}$ indicates that the field-sensitivity of a magnetic phase transition is inversely proportional to the maximum change of ΔS during heating or cooling. This indicates that high field-sensitivity results in lower ΔS, while a lower field-sensitive (where the phase transition is more easily driven by temperature) MPT with a relative smaller change in ΔM can result in a relatively large ΔS. This type of temperature-induced MPT usually results in sharp (narrower) $\Delta S(T)$ peaks[22,23] (associated with a significant contribution from the structural entropy change) during heating or cooling with a poor reversibility in ΔS due to the low field-sensitivity that hardly overcomes the usually large thermal hysteresis ΔT_{hyst}. Assuming that the ΔT_{hyst} connected with the structural compatibility at the martensitic to austenitic transformation[19,20] remains invariant as observed in the present studied system, a good field-sensitivity of the MPT is very important to realize a larger reversible ΔS (hereon referred to as $|\Delta S_{rev}|$). This is the portion of the total entropy change that can be exploited in cyclic magnetic cooling applications. It is typically considered and verified for different systems that the ΔS follows a power-law dependence with magnetic field [$\Delta S \propto (\mu_0 H)^n$].[24,25] Law *et al.*[25] developed a quantitative criterion for determining the order of magnetic phase transitions and also verified the criterion for different classes of materials, according to which the field exponent $n^{max} > 2$ is a characteristic feature of first-order phase transitions. Adopting a mean field approach, the same group of authors have recently developed a model that can capture the above-mentioned criterion for inverse magnetocaloric materials by introducing a cross coupling magnetovolume energy term with a magnetovolume coupling constant β.[26] For a finite value of β (other than zero), the model can result in a negative slope in the $\mu_0 H/M$ vs M^2 consistent with Banerjee's criterion for first-order phase transitions.[27] The model-generated data indicate that for a smaller value of β the overshoot of n^{max} above 2 is negligible, and n^{max} progressively increases above 2 with increasing β. Therefore, to realize a first-order phase transition with a signature of $n^{max} > 2$, a significant magnetovolume coupling (i.e., spin–lattice coupling) is required that can result in a field induced MPT, i.e., a metamagnetic transition. Since the field-induced MPT is responsible for the ΔS, the variation of the field sensitivity of the MPT is expected to have a signature in n^{max}.

It has been found in the present study that chemical substitution (acting as a positive chemical pressure) or application of hydrostatic pressure results in a substantial modification of the field-sensitivity of the MPT in boron-substituted Ni–Mn–In-based Heusler alloys. A drastic change in $|\Delta S_{rev}|$ has been observed as a result, although ΔT_{hyst} is found to be almost composition-independent. The possible origin of the variation in the field-sensitivity of the MPT has been discussed based on the experimental results. A clear correlation has been observed between n^{max} and the field-sensitivity of the MPT.

$Ni_{50}Mn_{34.8}In_{15.2-x}B_x$ ($x = 1$, 2, 3, and 4) samples were prepared using conventional arc-melting of the constituent elements Ni, Mn, and In (purity better than 99.9%) and boron (99.5% pure) under ultra-high purity Ar atmosphere. The samples were annealed inside evacuated quartz tubes under partially backfilled Ar ($p \sim 200$ mbar) atmosphere for 24 h at 850 °C followed by furnace cooling. Room-temperature x-ray diffraction measurements of the samples were performed in a Philips X'Pert Pro MPD diffractometer using Cu K_α radiation. The structural refinement of the XRD data was carried out using the Jana2006 software.[28] The magnetization measurements were carried out in a Quantum Design MPMS 3 magnetometer for the temperature interval of 2–400 K with applied magnetic fields up to $\mu_0 H = 7$ T. Magnetic measurements under hydrostatic pressure (p) were performed in a home-made BeCu piston-cylinder pressure cell. Mineral oil was used as the pressure transmitting medium. The values of the applied pressure (p) were determined based on the shift of the superconducting transition temperature of Sn (used as a reference manometer, $T_C \sim 3.72$ K at ambient pressure and field of approximately 5G).[29] Isofield $M(T)$ data have been used for calculating ΔS employing the Maxwell relation,[30]

$$\Delta S(T, \mu_0 H) = \sum_j \frac{M_{j+1}(T_{j+1}, \mu_0 H) - M_j(T_j, \mu_0 H)}{T_{j+1} - T_j} \Delta \mu_0 H,$$

where M_{j+1} (T_{j+1}, $\mu_0 H$) and M_j (T_j, $\mu_0 H$) represent the values of magnetization in a magnetic field $\mu_0 H$ at temperatures T_{j+1} and T_j, respectively. The reversible $|\Delta S_{rev}|$ is estimated considering the overlap region of the temperature-dependent entropy change curves on heating and cooling.[31] Differential scanning calorimetry (DSC) measurements were carried out using a DSC25 (TA Instruments) with a temperature ramp rate of 10 K/min during heating and cooling.

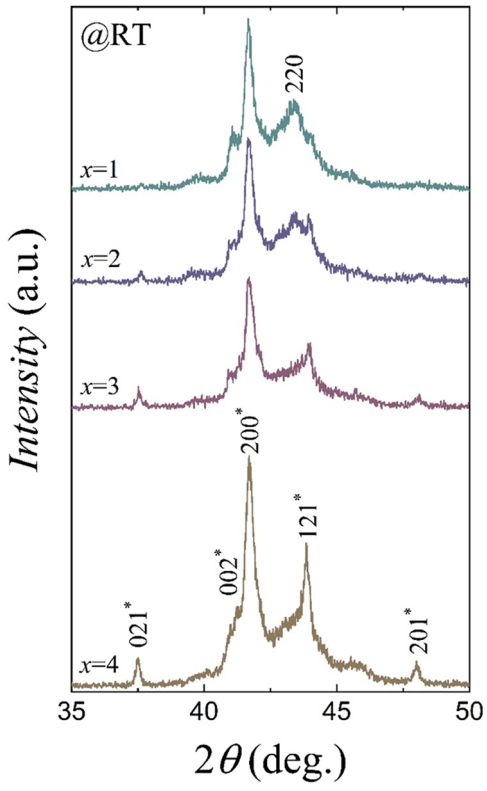

FIG. 1. Room-temperature XRD patterns for $Ni_{50}Mn_{34.8}In_{15.2-x}B_x$. The Miller indices of the monoclinic martensitic and cubic austenitic phases are indicated with and without an asterisk, respectively.

The room-temperature XRD patterns are shown in Fig. 1 for all the studied compositions. A modulated monoclinic martensitic structure (space group $P2/m$) has been detected for $x = 3$ and 4, similar to that reported in Ref. 19. However, the coexistence of austenitic $L2_1$-type cubic structure (space group $Fm\bar{3}m$) together with traces of martensitic phase has been identified for the composition with $x = 1$ and 2. The lattice parameters for $x = 1$ were found to be $a_0 = 5.8634$ Å for cubic austenitic phase and $a = 4.3063$ Å, $b = 5.6320$ Å, $c = 4.2143$ Å, and $\beta = 91.8339°$ for martensitic phase. The middle eigenvalue (λ_2) of the transformation matrix between martensitic and austenitic structures plays a crucial role to determine the structural compatibility associated with the phase transformation. The value of λ_2 closer to 1 indicates a better structural compatibility. $\lambda_2 \rightarrow 1$ usually results in a reduction of thermal hysteresis associated with a first-order phase transformation. The estimated value of λ_2 for $x = 1$ is 1.0076 (the deviation from 1 is 0.76%), indicating a good structural compatibility between monoclinic and cubic crystal structures. The details for examining the structural compatibility can be found in the supplementary material, S1.

The temperature-dependent magnetization (M) at ambient pressure and with the application of hydrostatic pressure ($p = 8.1$ kbar) for the $x = 1$ composition in the presence of a 7 T magnetic field is shown

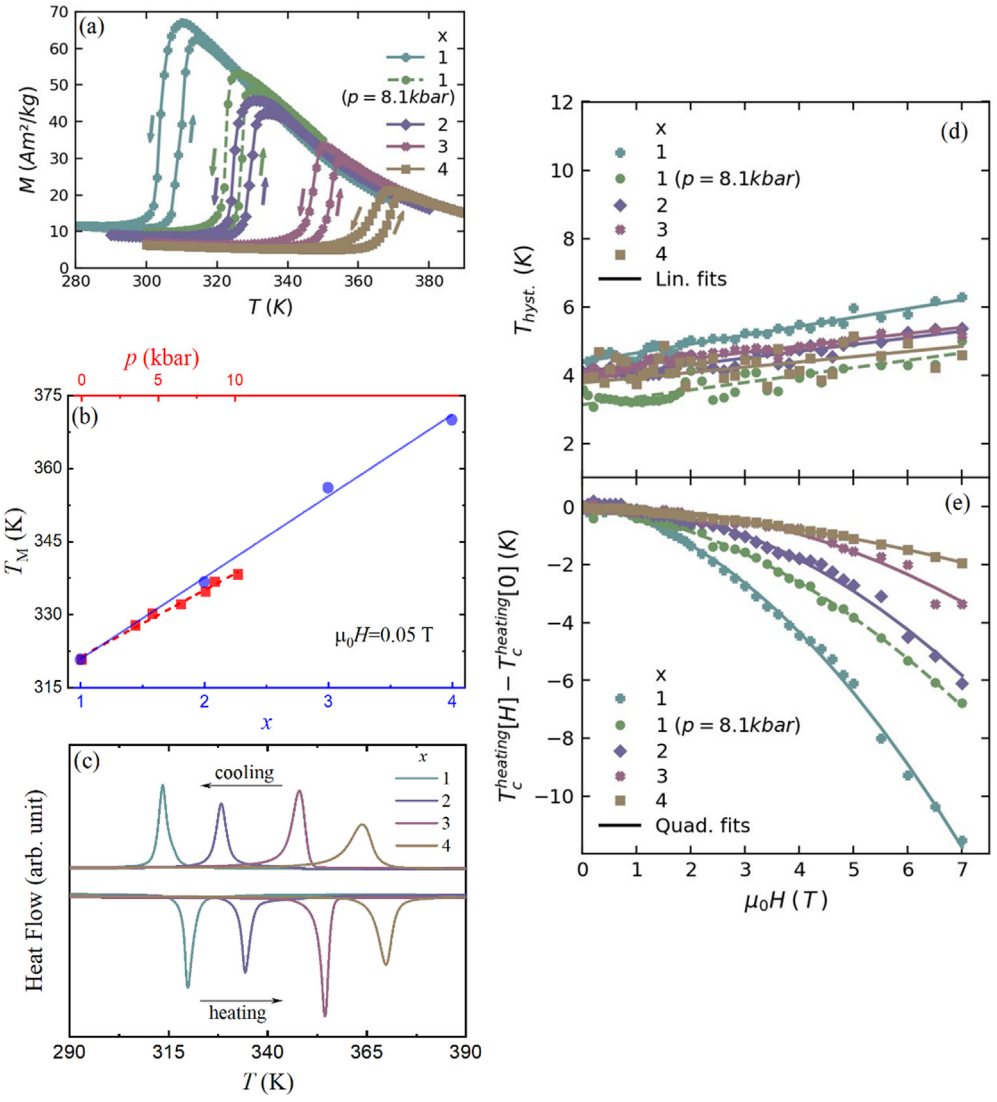

FIG. 2. (a) Temperature dependence of the magnetization during heating and cooling in the presence of $\mu_0 H = 7$ T for $x = 1$, 2, 3, and 4. $M(T)$ with the application of hydrostatic pressure $p = 8.1$ kbar and $\mu_0 H = 7$ T for $x = 1$ is shown by symbols connected with a dashed line. (b) Variations of T_M as a function of compositions (x) and pressure (p) for $x = 1$ as detected in the $M(T)$ measurement in the presence of $\mu_0 H = 0.05$ T. (c) DSC heat flow curves as a function of temperature measured at a rate of 10 K/min during heating and cooling. (d) Variations of thermal hysteresis (ΔT_{hyst}) as a function of applied magnetic field ($\mu_0 H$) at ambient pressure for different compositions and with the application of hydrostatic pressure $p = 8.1$ kbar for $x = 1$. (e) The magnetic field-induced shifts in T_M are shown for different compositions. The modification of T_M in the presence of $p = 8.1$ kbar for $x = 1$ is plotted by symbols connected with a dashed line.

in Fig. 2(a). A typical MPT from a low moment martensitic to ferromagnetic-type austenitic phase has been observed during heating and vice versa during cooling. Substitution of smaller B atoms for In ($R_B \sim 0.098$ and $R_{In} \sim 0.1663$ nm)[32] in $Ni_{50}Mn_{34.8}In_{15.2-x}B_x$ acts as a positive chemical pressure, shifting T_M toward higher temperatures. This is comparable to the effect of hydrostatic pressure, which stabilizes the lower-volume martensitic phase to higher temperatures resulting in an increase in the phase transition temperature with increasing pressure. The increase in T_M for B-substituted Heusler alloys was previously documented in the literature in $Ni_2Mn(GaB)$,[33] $Ni_{50}Mn_{36.5}Sb_{13.5-x}B_x$,[34] and $Ni_{50}Mn_{35}In_{15-x}B_x$.[35] A decrease of T_M is also reported for $Ni_{50}Mn_{35}In_{15-x}B_x$ with boron concentration below 1%.[36,37] The local distortion in the electronic structure likely reduces T_M through the stabilization of the austenitic phase for $x < 1$.[36] The increase in T_M for $x > 1$ is associated with the reduction of the crystal cell volume that stabilizes the martensitic phase.[36] The composition- and pressure-dependent (for $x = 1$) variations in T_M ($\mu_0 H = 0.05$ T) are shown in Fig. 2(b) (similar plot for $x = 2$ can be found in the supplementary material, S2). The observed thermal hysteresis, ΔT_{hyst}, between the heating and cooling $M(T)$ curves is a characteristic feature of the first-order nature of MPTs. The sharp endothermic/exothermic peaks during heating/cooling cycles observed in the DSC heat flow curves shown in Fig. 2(c) confirm the first-order character of the MPT. The composition-dependent variation of the transition entropy estimated from DSC data are included in the supplementary material, S3.

Magnetic field-dependent variation of the thermal hysteresis, ΔT_{hyst}, for all studied compositions are shown in Fig. 2(d). The substitution of B has a marginal impact on ΔT_{hyst}. The observed ΔT_{hyst} is below 5 K at low field, indicating a good structural compatibility at the MPT, consistent with earlier studies on In-based Heusler alloys.[19,20] ΔT_{hyst} increases almost linearly with increasing $\mu_0 H$ as reported for Ni–Mn–In and Ni–Mn–In–Co Heusler alloys.[38,39] Although ΔT_{hyst}

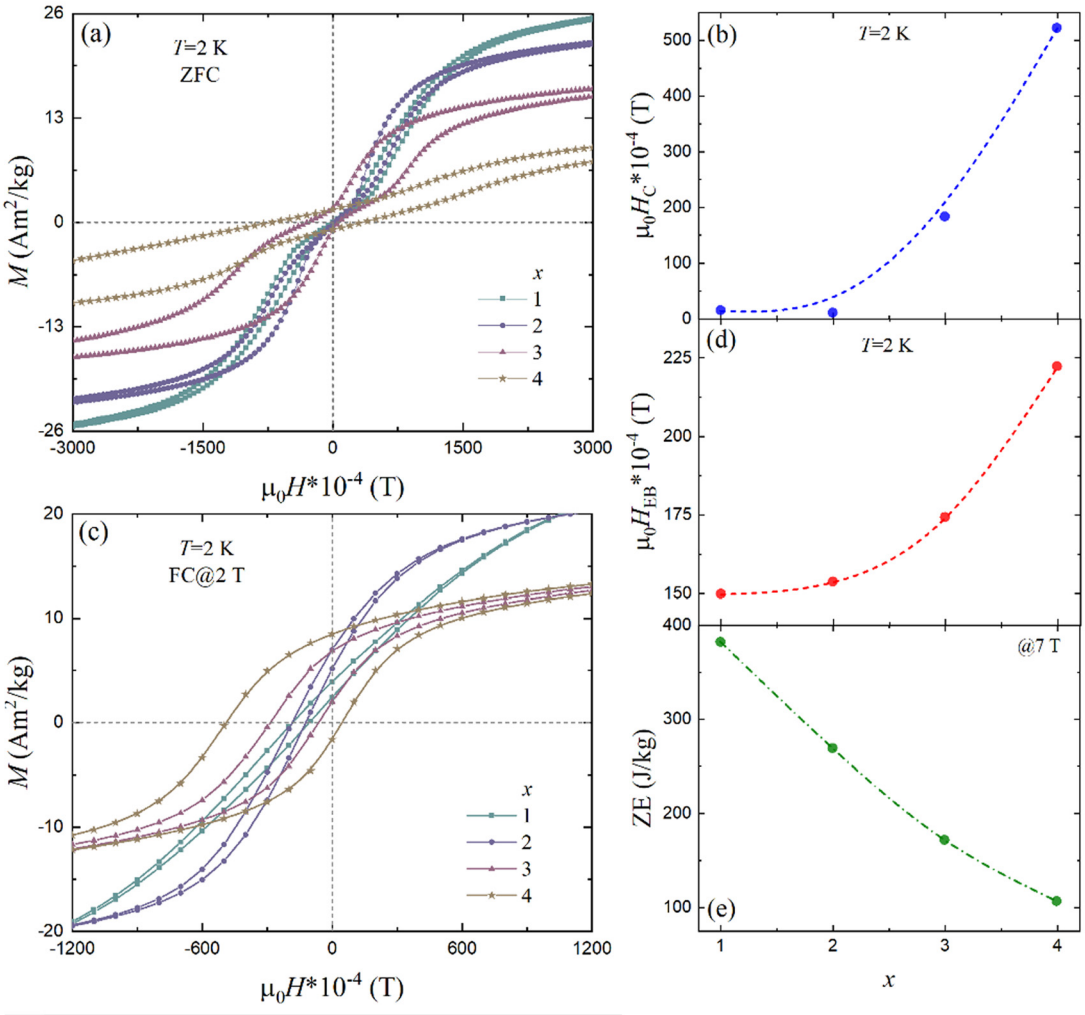

FIG. 3. (a) Zero-field-cooled (ZFC) $M(\mu_0 H)$ loop at 2 K and (b) corresponding coercivity ($\mu_0 H_C$) as a function of composition. (c) The shift of the origin in field-cooled (FC) $M(\mu_0 H)$ loops indicating the exchange-bias phenomena. (d) Composition-dependent exchange-bias field ($\mu_0 H_E$) at 2 K are shown. (e) Variation in Zeeman energy (ZE) as a function of composition estimated for $\mu_0 H = 7$ T.

stays nearly constant, a pronounced variation in the field-sensitivity of T_M has been observed depending on B concentration or hydrostatic pressure (p), as depicted in Fig. 2(e). The field-sensitivity in T_M decreases significantly with increasing B substitution and application of p. Instead of a linear field dependence, T_M varies more quadratically with $\mu_0 H$.

As discussed earlier, the competition between the two most significant energies, ZE and MAE, is responsible for the field-sensitivity of T_M. To examine the variation of the MAE with B concentration, zero-field-cooled (ZFC) $M(\mu_0 H)$ loop measurements have been performed at 2 K, the plots of which are shown in Fig. 3(a). A double-shifted hysteresis loop has been detected for all studied compositions, similar to that observed in Heusler alloys exhibiting exchange-bias (EB).[40–42] Interestingly, the magnetic coercivity increases with increasing B substitution, as depicted in Fig. 3(b). The increase in coercive field ($\mu_0 H_C$) clearly indicates that the magnetocrystalline anisotropy energy, MAE, in the martensitic phase is increasing with increasing B concentration. A large MAE is expected to result in a larger EB due to the strong interface coupling between anisotropic antiferromagnetic and FM phases.[43] This is consistent with the observed enhanced EB with increasing B content. The plots of field-cooled (FC) $M(\mu_0 H)$ EB-loops at 2 K and corresponding exchange-bias field ($\mu_0 H_E$) as a function of B concentration are shown in Figs. 3(c) and 3(d), respectively. The composition-dependent variation in Zeeman energy [$ZE = \Delta M^*(\mu_0 H)$] for $\mu_0 H = 7$ T [estimated from the data as plotted in Fig. 2(a)] is shown in Fig. 3(e). The ZE decreases with increasing B substitution. However, an increase in the MAE has been observed for higher B concentrations [see Fig. 3(b)]. This indicates that a larger ZE is required to overcome the enhanced MAE for higher B concentrations. As ΔM is reduced with increasing B concentration, a higher magnetic field is required to overcome the enhanced MAE and, accordingly, the field-sensitivity of the MPT decreases for higher B concentrations.

The temperature-dependent variation of the isothermal entropy change (ΔS) for $\Delta\mu_0 H = 7$ T during heating and cooling are shown in Figs. 4(a)–4(e) for all studied compositions (including application of $p = 8.1$ kbar for $x = 1$). At higher temperature, the second-order magnetic phase transition (FM-paramagnetic) occurring in the austenitic phase gives rise to conventional MCE, which is fully reversible. A relatively large inverse MCE has been observed associated with the first-order MPT. The corresponding reversible entropy change ($|\Delta S_{rev}|$) is

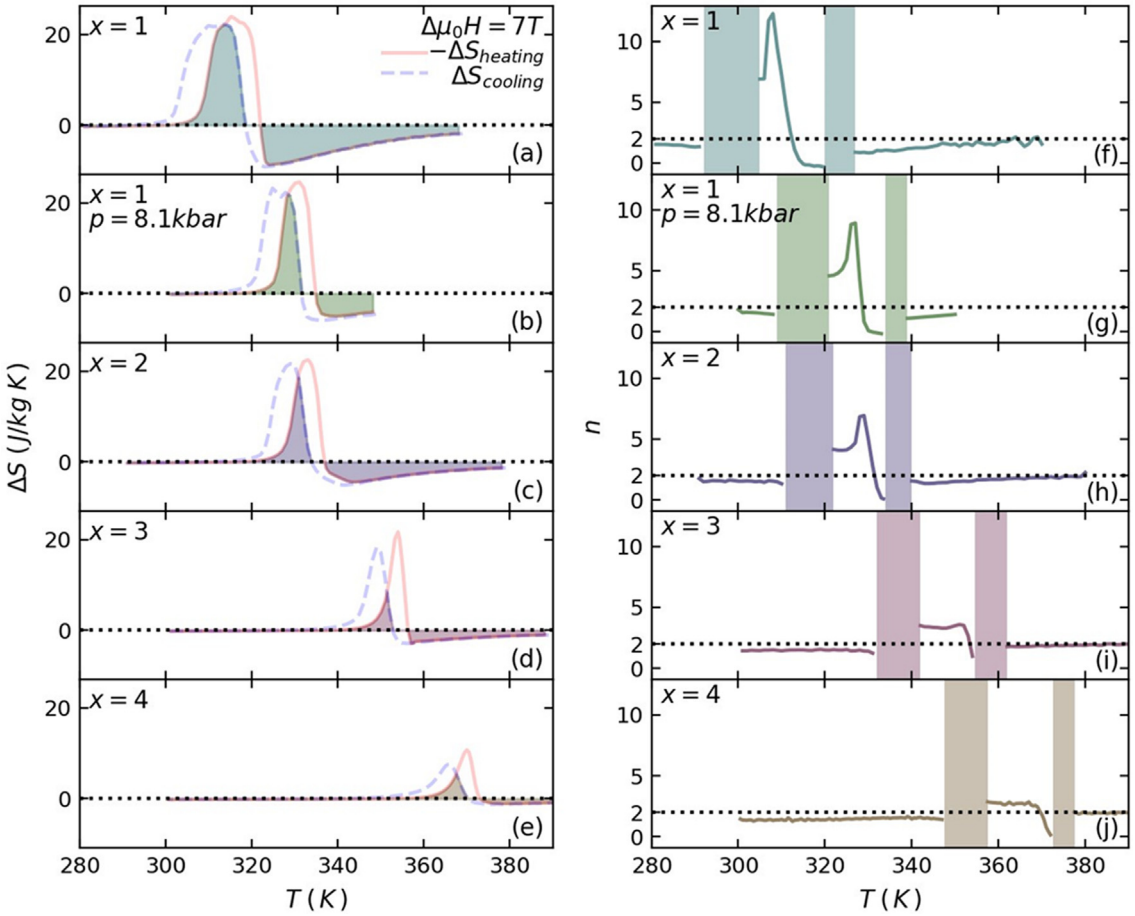

FIG. 4. (a)–(e) Composition- and pressure-dependent (for $x = 1$ with $p = 8.1$ kbar) variations of isothermal entropy change $|\Delta S|$ as a function of temperature during heating and cooling for $\Delta\mu_0 H = 7$ T. The reversible region of ΔS ($|\Delta S_{rev}|$) is highlighted by shades. (f)–(j) Temperature-dependent variations of field exponent n for different compositions and with application of $p = 8.1$ kbar for $x = 1$ as estimated for a magnetic field change of $\Delta\mu_0 H = 7$ T during heating.

represented as the shaded area. $|\Delta S_{rev}|$ decreases with increasing B concentration/application of p as the MPT becomes less field sensitive. The strongest field-sensitivity around the MPT was observed for $x = 1$, where $|\Delta S_{rev}|$ reaches a value of 21.48 J/kg K for $\Delta\mu_0 H = 5$ T. This $|\Delta S_{rev}|$ is comparable or even larger than the values reported for the best-known In-based (e.g., $|\Delta S_{rev}| = 18.9$ and 16.4 J/kg K for $\Delta\mu_0 H = 5$ T as reported for $Ni_{50.7}Mn_{33.4}In_{15.6}V_{0.3}$ (Ref. 19) and $Ni_{46}Co_3Mn_{35}Cu_2In_{14}$,[44] respectively) and Sn-based Heusler alloys (e.g., $|\Delta S_{rev}| = 19.3$ and 18.7 J/kg K for $\Delta\mu_0 H = 5$ T reported for $Ni_{43}Co_6Mn_{40}Sn_{11}$[45] and $Ni_{41}Ti_1Co_9Mn_{39}Sn_{10}$[46] exhibiting a giant inverse MCE). The details of $\Delta S(T)$ and associated $|\Delta S_{rev}|$ up to $\Delta\mu_0 H = 7$ T for all studied compositions (including application of $p = 8.1$ kbar for $x = 1$) are included in the supplementary material, S4.

The local field exponent, n, has been estimated considering the following equation:[24,25]

$$n = \frac{dln|\Delta S|}{dln(\mu_0 H)}.$$

The temperature dependence of n for $\mu_0 H = 7$ T is shown in Figs. 4(f)–4(j). Further details in the variation of $n(T, H)$ can be found in the supplementary material, S5. For all studied compositions, the observed value of n is greater than 2 in the vicinity of the MPT, indicating the first-order nature of the phase transition. However, the overshoot of n above 2 is more significant for lower B concentrations. The field-sensitivity-dependence [i.e., $dT_M/d(\mu_0 H)$] of n^{max} at $\mu_0 H = 7$ T for all compositions and for x = 1 under hydrostatic pressure is plotted in Fig. 5. An interesting correlation has been observed between n^{max} and $dT_M/d(\mu_0 H)$. A stronger field-sensitive MPT [large $dT_M/d(\mu_0 H)$] results in a larger value of n^{max} and vice versa. This feature indicates that "Anzai and Ozawa"-type temperature-induced MPT as commonly observed in the MnTX system (T = Co, Ni and X = Ge, Si; where field-induced MPT is often barely visible)[47,48] should result in small n^{max} due to the low field-sensitivity of the MPT. In other words, large n^{max} is a characteristic of strong field-sensitive MPT (strong spin–lattice coupling[1]), whereas the temperature starts to dominate over the magnetic field to drive the MPT (weak spin–lattice coupling[22]) for lower n^{max}.

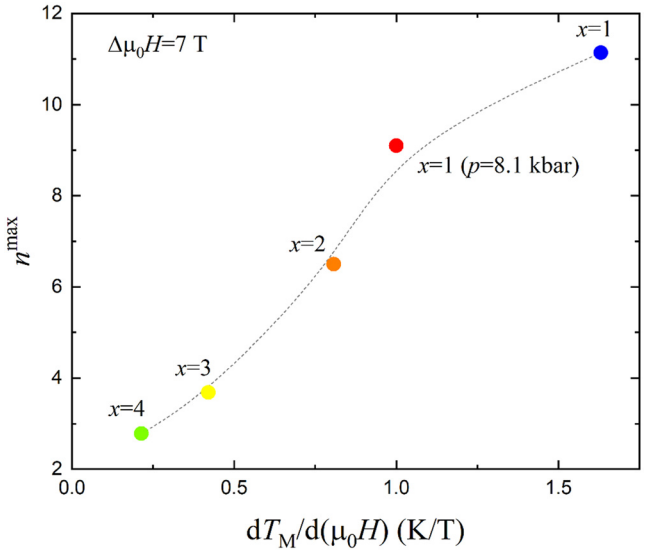

FIG. 5. Dependence of n^{max} with field-sensitivity of MPT [$dT_M/d(\mu_0 H)$] for different compositions and application of hydrostatic pressure for $x = 1$ are shown for $\mu_0 H = 7$ T.

In conclusion, studies on B-substituted In-based Heusler alloys indicate that the martensitic phase transition temperature, T_M, can be effectively adjusted by chemical substitution or application of hydrostatic pressure. Concomitantly, the nature of the field-induced MPT is drastically modified. The field-sensitivity of the MPT decreases with increasing B concentration or application of hydrostatic pressure. It has been found that two competing energies, namely the ZE and the MAE, driving the MPT follow opposite trends depending on B concentration (the effect is identical to that of p). Large MAE is conducive to exchange-bias properties, but it has an adverse effect on the field-induced magnetocaloric properties. A higher magnetic field is required to overcome a large MAE and drive the MPT. In this case, a reduction in the reversibility of $|\Delta S_{rev}|$ is expected, which has been observed for higher B concentrations or application of p. The observed larger local magnetic field exponent n^{max} for higher field-sensitive MPT ($x = 1$) indicates a stronger first-order character of the phase transition, which has the potential to exhibit a better reversible $|\Delta S_{rev}|$.

See the supplementary material for the details of the structural compatibility condition, pressure-dependent shift of T_M for $x = 2$, composition-dependent variation of transition entropy, reversible entropy change up to $\Delta\mu_0 H = 7$ T for all studied compositions, and 2D color-contour-plot of the variation field exponent $n(T, H)$.

This work was carried out in the framework of the Joint Lab BiBer and was supported by the BMBF joint project DiProMag—Digitalization of a process chain for the production, characterization, and prototypical application of magnetocaloric alloys, here the contribution of Bielefeld University: FKZ 13XP5 120B, with the objective of producing magnetocaloric Heusler compounds and ontology development. The authors thank Laila Bondzio and Andreas Hütten (Faculty of Physics, Bielefeld University, Germany) for providing the access to the DSC instrument.

AUTHOR DECLARATIONS

Conflict of Interest

The authors have no conflicts to disclose.

Author Contributions

Chris Taake: Data curation (equal); Formal analysis (equal); Investigation (equal); Software (lead); Writing – original draft (equal); Writing – review & editing (equal). **Tapas Samanta:** Conceptualization (equal); Data curation (equal); Formal analysis (equal); Investigation (equal); Methodology (equal); Visualization (lead); Writing – original draft (lead); Writing – review & editing (lead). **Luana Caron:** Conceptualization (equal); Funding acquisition (lead); Investigation (equal); Resources (lead); Supervision (lead); Visualization (equal); Writing – original draft (equal); Writing – review & editing (equal).

DATA AVAILABILITY

The data that support the findings of this study are available from the corresponding author upon reasonable request.

REFERENCES

[1]J. Liu, T. Gottschall, K. P. Skokov, J. D. Moore, and O. Gutfleisch, Nat. Mater. **11**, 620 (2012).
[2]V. K. Sharma, M. K. Chattopadhyay, K. H. B. Shaeb, A. Chouhan, and S. B. Roy, Appl. Phys. Lett. **89**, 222509 (2006).
[3]R. Kainuma, Y. Imano, W. Ito *et al.*, Nature **439**, 957 (2006).
[4]Y. Zhang, W. Hao, C. Hu, X. Wang, X. Zhang, and L. Li, Adv. Funct. Mater. **33**, 2310047 (2023).
[5]S. Huang, E. Dastanpour, S. Schönecker *et al.*, Appl. Phys. Lett. **123**, 044103 (2023).
[6]Y. Zhang, P. Xu, J. Zhu, S. Yan, J. Zhang, and L. Li, Mater. Today Phys. **32**, 101031 (2023).
[7]J. Y. Law and V. Franco, APL Mater. **9**, 080702 (2021).
[8]L. Li and M. Yan, J. Mater. Sci. Technol. **136**, 1–12 (2023).
[9]Y. Zhang, Y. Tian, Z. Zhang, Y. Jia, B. Zhang, M. Jiang, J. Wang, and Z. Ren, Acta Mater. **226**, 117669 (2022).
[10]J. Y. Law and V. Franco, Handb. Phys. Chem. Rare Earths **64**, 175 (2023).
[11]I. Dubenko, T. Samanta, A. K. Pathak, A. Kazakov, V. Prudnikov, S. Stadler, A. Granovsky, A. Zhukov, and N. Ali, J. Magn. Magn. Mater. **324**, 3530 (2012).
[12]T. Samanta, C. Taake, L. Bondzio, and L. Caron, J. Phys. Energy **5**, 044002 (2023).
[13]T. Krenke, E. Duman, M. Acet, E. F. Wassermann, X. Moya, L. Mañosa, and A. Planes, Nat. Mater. **4**, 450 (2005).
[14]A. K. Pathak, M. Khan, I. Dubenko, S. Stadler, and N. Ali, Appl. Phys. Lett. **90**, 262504 (2007).
[15]J. Hao, F. Hu, J. T. Wang, F. R. Shen, Z. Yu, H. Zhou, H. Wu, Q. Huang, K. Qiao, J. Wang, J. He, L. He, J. R. Sun, and B. Shen, Chem. Mater. **32**, 1807 (2020).
[16]T. Samanta, B. Weise, L. Beyer, and M. Krautz, J. Appl. Phys. **129**, 023901 (2021).
[17]S. Anzai and K. Ozawa, Phys. Rev. B **18**, 2173 (1978).
[18]T. Krenke, M. Acet, E. F. Wassermann, X. Moya, L. Mañosa, and A. Planes, Phys. Rev. B **73**, 174413 (2006).
[19]J. Liu, X. You, B. Huang, I. Batashev, M. Maschek, Y. Gong, X. Miao, F. Xu, N. van Dijk, and E. Brück, Phys. Rev. Mater. **3**, 084409 (2019).
[20]P. Devi, C. Salazar Mejía, L. Caron, S. Singh, M. Nicklas, and C. Felser, Phys. Rev. Mater. **3**, 122401(R) (2019).
[21]H. E. Karaca, I. Karaman, B. Basaran, Y. Ren, Y. I. Chumlyakov, and H. J. Maier, Adv. Funct. Mater. **19**, 983 (2009).
[22]L. Caron, N. T. Trung, and E. Brück, Phys. Rev. B **84**, 020414(R) (2011).
[23]T. Samanta, D. L. Lepkowski, A. Us Saleheen, A. Shankar, J. Prestigiacomo, I. Dubenko, A. Quetz, I. W. H. Oswald, G. T. McCandless, J. Y. Chan, P. W. Adams, D. P. Young, N. Ali, and S. Stadler, Phys. Rev. B **91**, 020401(R) (2015).
[24]T. D. Shen, R. B. Schwarz, J. Y. Coulter, and J. D. Thompson, J. Appl. Phys. **91**, 5240 (2002).
[25]J. Y. Law, V. Franco, L. M. Moreno-Ramírez, A. Conde, D. Y. Karpenkov, I. Radulov, K. P. Skokov, and O. Gutfleisch, Nat. Commun. **9**, 2680 (2018).
[26]L. M. Moreno-Ramírez, J. Y. Law, S. S. Pramana, A. K. Giri, and V. Franco, Results Phys. **22**, 103933 (2021).
[27]S. K. Banerjee, Phys. Lett. **12**, 16 (1964).
[28]V. Petricek, L. Palatinus, J. Plasil, and M. Dusek, Z. Kristallogr. **238**, 271 (2023).
[29]A. Eiling and J. S. Schilling, J. Phys. F **11**, 623 (1981).
[30]L. Caron, N. B. Doan, and L. Ranno, J. Phys. **29**, 075401 (2017).
[31]B. Kaeswurm, V. Franco, K. P. Skokov, and O. Gutfleisch, J. Magn. Magn. Mater. **406**, 259 (2016).
[32]W. B. Pearson, *The Crystal Chemistry and Physics of Metals and Alloys* (Wiley-Interscience, New-York, 1972).
[33]B. R. Gautam, I. Dubenko, A. K. Pathak, S. Stadler, and N. Ali, J. Phys. **20**, 465209 (2008).
[34]H. Luo, F. Meng, Q. Jiang, H. Liu, E. Liu, G. Wu, and Y. Wang, Scr. Mater. **63**, 569 (2010).
[35]T. Samanta, A. Us Saleheen, D. L. Lepkowski, A. Shankar, I. Dubenko, A. Quetz, M. Khan, N. Ali, and S. Stadler, Phys. Rev. B **90**, 064412 (2014).
[36]S. Pandey, A. Quetz, I. D. Rodionov, A. Aryal, M. I. Blinov, I. S. Titov, V. N. Prudnikov, A. B. Granovsky, I. Dubenko, S. Stadler, and N. Ali, J. Appl. Phys. **117**, 183905 (2015).
[37]M. Blinov, A. Aryal, S. Pandey *et al.*, Phys. Rev. B **101**, 094423 (2020).
[38]T. Gottschall, K. P. Skokov, D. Benke, M. E. Gruner, and O. Gutfleisch, Phys. Rev. B **93**, 184431 (2016).
[39]L. Pfeuffer, T. Gottschall, T. Faske, A. Taubel, F. Scheibel, A. Y. Karpenkov, S. Ener, K. P. Skokov, and O. Gutfleisch, Phys. Rev. Mater. **4**, 111401(R) (2020).
[40]M. Khan, I. Dubenko, S. Stadler, and N. Ali, Appl. Phys. Lett. **91**, 072510 (2007).
[41]A. K. Pathak, M. Khan, B. R. Gautam, S. Stadler, I. Dubenko, and N. Ali, J. Magn. Magn. Mater. **321**, 963 (2009).
[42]A. K. Nayak, R. Sahoo, K. G. Suresh, A. K. Nigam, X. Chen, and R. V. Ramanujan, Appl. Phys. Lett. **98**, 232502 (2011).
[43]J. Nogués, J. Sort, V. Langlais, V. Skumryev, S. Suriñach, J. S. Muñoz, and M. D. Baró, Phys. Rep. **422**, 65 (2005).
[44]Z. Li, J. Yang, D. Li, Z. Li, B. Yang, H. Yan, C. F. Sánchez-Valdés, J. L. S. Llamazares, Y. Zhang, C. Esling, X. Zhao, and L. Zuo, Adv. Electron. Mater. **5**, 1800845 (2019).
[45]Y. H. Qu, D. Y. Cong, S. H. Li, W. Y. Gui, Z. H. Nie, M. H. Zhang, Y. Ren, and Y. D. Wang, Acta Mater. **151**, 41 (2018).
[46]Y. H. Qu, D. Y. Cong, X. M. Sun, Z. H. Nie, W. Y. Gui, R. G. Li, Y. Ren, and Y. D. Wang, Acta Mater. **134**, 236 (2017).
[47]T. Samanta, D. L. Lepkowski, A. U. Saleheen, A. Shankar, J. Prestigiacomo, I. Dubenko, A. Quetz, I. W. H. Oswald, G. T. McCandless, J. Y. Chan, P. W. Adams, D. P. Young, N. Ali, and S. Stadler, J. Appl. Phys. **117**, 123911 (2015).
[48]T. Samanta, I. Dubenko, A. Quetz, S. Stadler, and N. Ali, J. Appl. Phys. **113**, 17A922 (2013).